Brain Tumour Detection using Double Multilayer Resilient Propagation Neural Network (MLRPNN)

D. Selvaraj* and R. Dhanasekaran**

In the proposed method, an automatic brain tumour segmentation and classification system is developed. The input image is preprocessed, segmented and features are extracted. Based on the extracted features, the input image is classified as cancerous or non-cancerous image using multilayer resilient propagation neural network classifier. In the preprocessing stage, noise is removed using median filter and the skull is stripped using morphological operators. Using thresholding technique and orthogonal polynomial transform, the skull stripped image is segmented into gray matter, white matter, cerebrospinal fluid and tumour. Then features like mean, variance, energy, and entropy are calculated. Later, multilayer resilient propagation neural network (MLRPNN) is trained with extracted features. A total of 150 images have been used, out of which 60 are used for training and remaining 90 images for testing. MLRPNN classifier classifies the input image to be cancer affected or normal based on features extracted. If the image is cancer affected, then type of cancer is detected as malign tumor or benign tumor using another MLRPNN Classifier. The performance of the proposed technique is validated and compared with the standard evaluation metrics such as sensitivity, specificity and accuracy values for neural network. The proposed method is compared with two standard methods KNN and FCM+NN. The obtained result depicts that the proposed classification method yields better results.

Keywords: Brain Segmentation, Feature Extraction, Neural Network, Brain Tumour.

1. Introduction

The primary goal of MRI brain image segmentation is to partition a given brain image into true anatomical structures representing such as grey matter, white matter, cerebrospinal fluid, skull and scalp. Later, the abnormalities in these tissues are detected. Identification and segmentation of brain tumor in magnetic resonance images is very crucial in medical diagnosis because it gives information related to anatomical structures as well as potential abnormal tissues necessary for treatment planning and patient follow-up. Precise segmentation of brain tumor is also useful for general modeling of pathological brains as well as the creation of pathological brain atlases [16, 17].There is a significant inter-patient variation of signal intensities for the same tissues [3]. Although there are several approaches for MRI Brain image segmentation : discriminate analysis [5], neural networks [6,7], clustering [4], brain atlases [8], knowledge-based techniques [9], shape-based models [10,11], morphological operators [12], multivariate principal component analysis [13], pixel based models like Expectation Maximization Algorithm [14], Multi-resolution edge detection [6] and statistical pattern recognition [15], to name a few. Precise segmentation and classification of abnormalities are still a challenging and complicated task because of inherent noise, partial volume effect, different shapes, locations and image intensities of different types of tumors.

Manual segmentation cannot be compared with the current high speed computing machines that allow us to visually observe the size and position of the superfluous tissues. Supervised segmentation methods have exhibited problems with reproducibility, due to significant intra and inter-observer variance introduced over multiple trials of training Furthermore; they are time consuming and require domain expertise. Whereas, the accuracy of unsupervised segmentation methods are less and depend upon input image. So these limitations suggest the need for a fully automatic method for segmentation.

*Department of Electronics and Communication Engineering, Sathyabama University, Chennai, Tamil Nadu -600119
**Syed Ammal Engineering College, Landhai, Tamil Nadu -623502
Emails: mails2selvaraj@yahoo

In this paper, we have presented an efficient detection technique for the tumor region in the Brain MRI images. Here, we have utilized the brain tissue segmentation technique that we have proposed in our previous research paper [1, 2, 19, 20]. In addition with that, we have detected the tumor region with the aid of the regionprops algorithm [18]. Subsequently, the features vectors of all the segmented regions of the brain MRI image are calculated. Then, the abnormality classification is carried out by means of multilayer resilient propagation neural network. The rest of this paper is organized as follows: section 2 presents our proposed Brain tissues segmentation technique. Extractions of features from the segmented tissues are explained in section 3. Section 4 explains the classification of the input image using MLRPNN. The detailed experimental results and discussions are given in section 5. At last, section 6 concludes the paper.

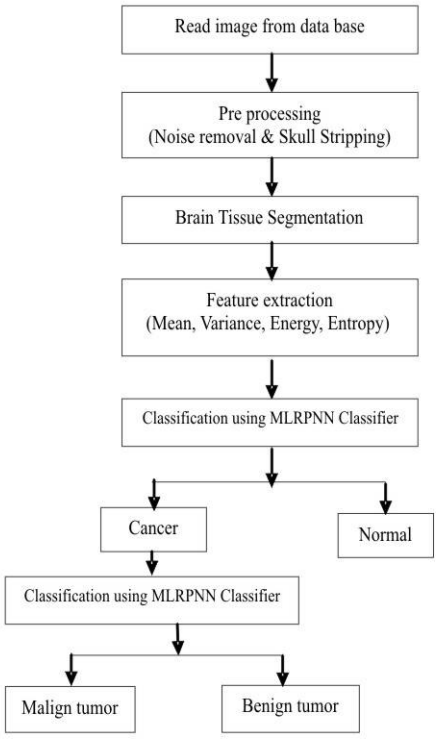

Fig. 1: Block diagram of proposed approach.

2. Proposed Method

The block diagram of the proposed technique is shown in Fig 1. Our proposed method consists of 4 phases namely preprocessing, segmentation, feature extraction and classification. In preprocessing phase, the noise is removed using median filter and the skull is stripped using morphological operators and thresholding technique. Later, the skull stripped image is segmented into gray matter and white matter using thresholding technique. Orthogonal polynomial transform is used to segment cerebrospinal fluid. After segmentation process, the features such as Mean, Variance, Energy and Entropy are extracted from the regions and given to the MLRPNN classifier for training. Later, the image is classified as tumourous or normal with the help of trained MLRPNN. Finally, the type of cancer is detected using another MLRPNN classifier.

The obtained experimental results by our proposed technique in our previous research paper [1, 2, 19, 20] are as shown in Fig 2 and Fig 3. Here, we have given all the outcomes of the input image with and without tumour region.

3. Feature Extraction from the Segmented Tissues

The analyzing methods have been done so far has used the values of pixels intensities, pixels coordinates and some other statistic features namely mean, variance or median, which have much error in determination process and low precision and efficiency in classification [19] . Here, the statistic features chosen are Mean M, Variance σ^2, Entropy E and Energy $E_{(E,V,D)}$ functions. The feature extraction process is carried out with some initial pre-processing. Each tissue segmented image is split into a limited number of blocks and the feature values are calculated for every block.

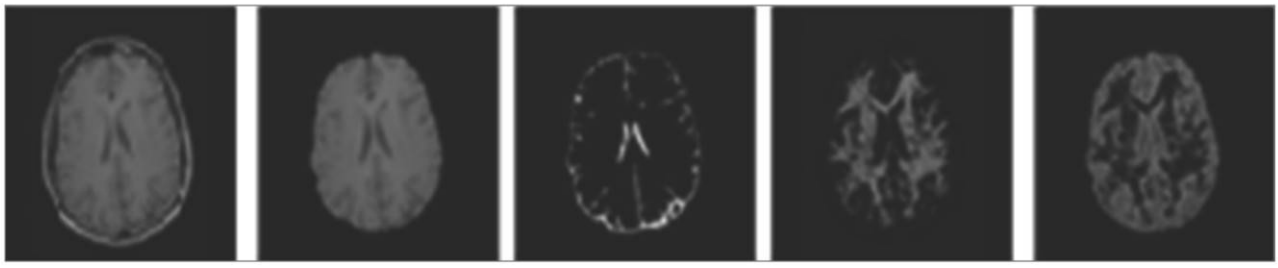

Fig. 2.1: Segmented results of Brain MRI without tumor. (a) Input Brain MRI image, (b) Skull stripped image, (c) Cerebrospinal fluid image, (d) White matter, (e) Gray matter

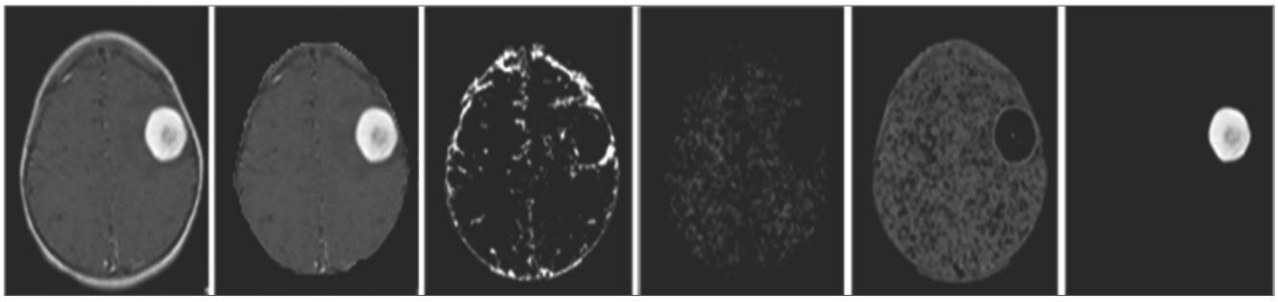

Fig. 2.2: Segmented results of Brain MRI with tumor. (a) Input Brain MRI image, (b) Skull stripped image, (c) Cerebrospinal fluid image, (d) White matter, (e) Gray matter, (f) Tumor region

The block diagram of the feature extraction process is given in Fig. 4. The initial steps are as follows:

- The neighbor blocks of the entire divided blocks are found
- The distance between all the neighbor blocks is found.
- The feature values of the blocks with distinct distance measure are found.
- The average value of all the computed blocks' distance is found.
- All the features in a vector are stored and fed as an input to the classifier.

Segmented Image Blocks Divided Image GM. The statistic feature's formula is depicted as below,

Mean, $$M = \frac{1}{mn}\sum_{i=1}^{m}\sum_{j=1}^{m} x(i,j) \quad (1)$$

Variance,

$$\sigma^2 = \frac{1}{mn}\sum_{i=1}^{m}\sum_{j=1}^{n} (x(i,j) - M)^2 \quad (2)$$

Entropy,

$$E = -\sum_{i}\sum_{j} x(i,j)\log x(i,j) \quad (3)$$

Energy, $$E_{(H,V,D)} = \sum_{i}\sum_{j} x(i,j)^2 \quad (4)$$

Selection of efficient features can reduce significantly the difficulty of the classifier design. The obtained trained feature is compared with the test sample feature obtained and classified as one of the extracted features. The training feature vector F_v is defined by combining all the extracted features like mean M, variance σ^2, entropy E and the energy $E_{(H,V,D)}$. In order to obtain the three wavelet energies, the Haar wavelet transform is applied to each blocks of brain MRI image. After a one level wavelet transform, a 4×4 pixel block is decomposed into four frequency bands of 2×2 coefficients. For example, the coefficients in horizontal band of one block are H_1, H_2, H_3, H_4, in vertical band V_1, V_2, V_3, V_4 and in diagonal band D_1, D_2, D_3 and D_4. Then horizontal energy E_H, vertical energy E_V and diagonal energy E_D are combined to attain the feature value of the energy. Feature Vector,

$$F_v = [f(M), f(\sigma^2), f(E), f(E_H), f(E_V), f(E_D)]$$

4. Brain Image Classification Using MLRPNN

The classifiers we have used here is MLRPNN. The general structure of MLRPNN is shown in fig. 3. In this network, the information moves in only one direction, forward from input layer to the output layer through the hidden layers. The network consists of 1 input layer with 24 neurons, 1 output layer with one neuron and 2 layers of hidden units with 10 neurons. The algorithm used to train the network is resilient propagation algorithm.

Each hidden node calculates the weighted sum of its inputs and applies a thresholding function to determine the output of the hidden node. The weighted sum of the inputs for hidden node Zh is calculated as:

$$Z_h = \sum_{i=0}^{n} W_{hi} x_i \quad (6)$$

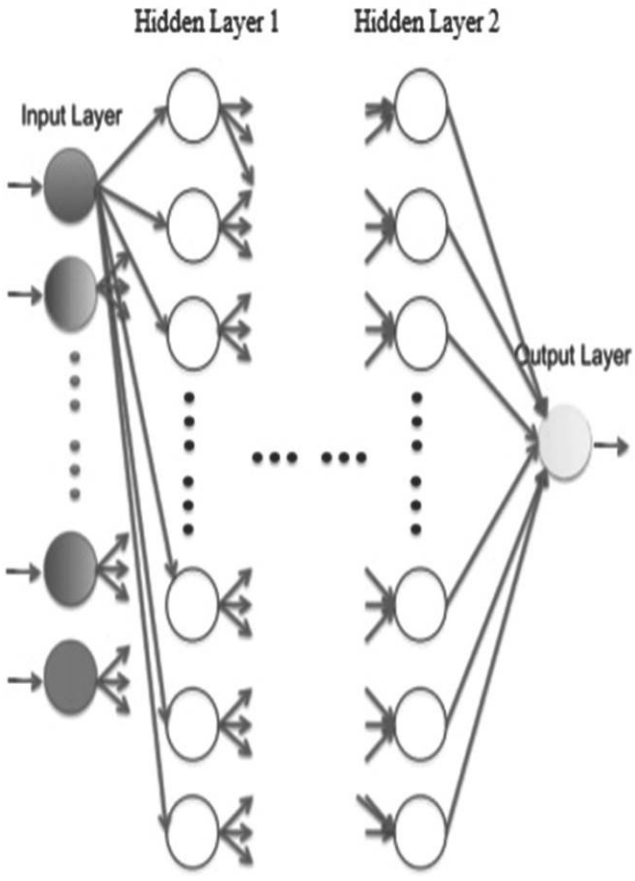

Fig. 3:
General Structure of MLRPNN

The thresholding function applied at the hidden node is a sigmoid function. The general form of the sigmoid function is

$$\text{Sigmoid}(a) = \frac{1}{1+e^{-a}} \tag{7}$$

The sigmoid function is also called as squashing function, because it squashes its input to a value between 0 and 1. At the hidden node, the sigmoid function is applied to the weighted sum of the inputs to the hidden node. So, the output of hidden node is given as,

$$Z_h = \text{Sigmoid}\left(\sum_{i=0}^{n} W_{hi} x_i\right) = \frac{1}{1+e^{-\sum_{i=0}^{n} W_{hi} x_i}} \tag{8}$$

Similar computation is done for the next hidden and output units. We have only one output unit in the output layer. So, the following sigmoid function (equation 9) is applied to the output unit.

$$y = \text{Sigmoid}\left(\sum_{h=0}^{N} V_h z_h\right) = \frac{1}{1+e^{-\sum_{h=0}^{N} V_h z_h}} \tag{8}$$

The algorithm used to train the neural network is resilient propagation algorithm [21]. This algorithm is the modified algorithm of standard back propagation algorithm. In this algorithm, the weight updating method of standard back propagation algorithm is modified. Resilient propagation algorithm (RPA) performs a direct adaption of weight step based on local gradient information. RPA considers only the sign of the derivative to indicate the direction of the weight update. The size of the weight change is determined by the update value.

$$\Delta W_{ij} = -\text{sign}\left(\frac{\partial E}{\partial W_{ij}}\right).\Delta_{ij} \tag{9}$$

Where, Δij is an update value which evolves during the learning process according to the following rule.

RPA Learning Rule:

$$\Delta_{ij}(t) = \begin{cases} \eta^{+}.\Delta_{ij}(t-1); if\ S_{ij} > 0 \\ \eta^{-}.\Delta_{ij}(t-1); if\ S_{ij} < 0 \\ \Delta_{ij}(t-1); Otherwise \end{cases} \tag{10}$$

Where, Δij is an update value which evolves during the learning process according to the following rule.

RPA Learning Rule:

Where,
$$S_{ij} = \frac{\partial E}{\partial W_{ij}}.(t-1).\frac{\partial E}{\partial W_{ij}}(t) \tag{11}$$
$$\eta^{+} = 1.2\ ;\ \eta^{-} = 0.5$$

RPA Weight Step Rule:

$$\Delta W_{ij}(t) = \begin{cases} -\Delta_{ij}(t); if\ R_{ij} > 0 \\ +\Delta_{ij}(t); if\ R_{ij} < 0 \\ 0 \quad ; Otherwise \end{cases} \tag{12}$$

Where, $R_{ij} = \frac{\partial E}{\partial W_{ij}}.(t)$

The weight update follow simple rule: if the derivative is positive (increasing error), the weight is decreased by its update value and if the derivative is negative, the update value is added.

5. Experimental Results and Discussions

We have presented a technique for segmentation and detection of pathological tissues (Tumor), normal tissues (White Matter and Gray Matter) and fluid (Cerebrospinal Fluid) from magnetic resonance (MR) images of brain with the help of composite feature vectors comprising of wavelet and statistical parameters. The proposed technique can successfully segment the tumors as well as the brain tissues, provided that theparameters are set properly. The proposed technique is designed for supporting the tumor detection in brain images with tumor and without tumor. The obtained experimental results from the proposed technique are given in Fig. 4 and Fig. 5. In fig. 4 and fig. 5, the segmented normal tissues (CSF, WM, GM) and pathological tissues (tumour) of MRI brain image with and without tumor is shown. The feature values calculated for these segmented tissues using block based feature extraction method is tabulated in table 1. The simulation result of neural network training dataset is as shown in Fig 6 to Fig 9.

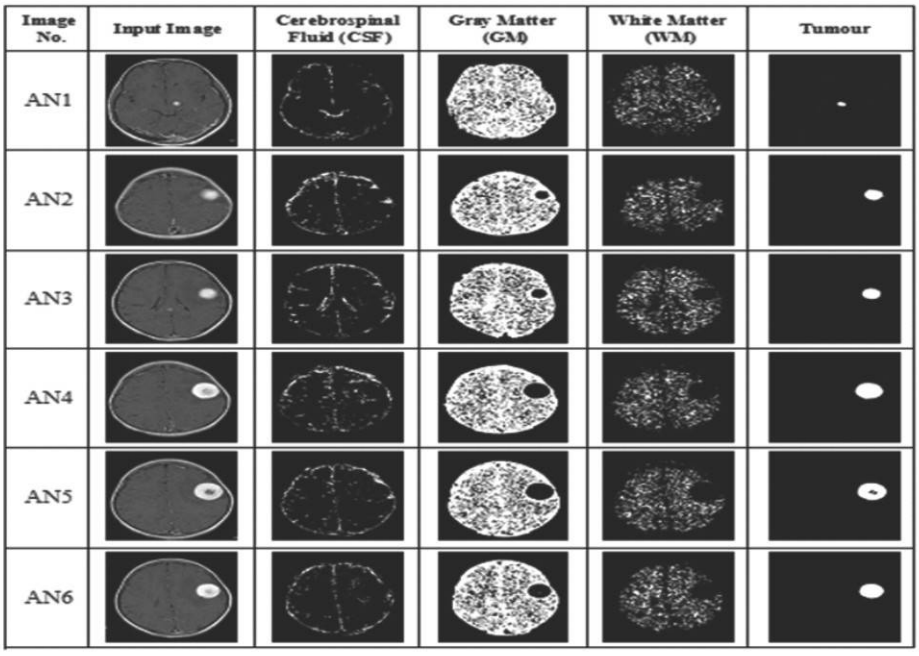

Fig. 4: Segmented normal tissues (CSF, GM, WM) and pathological Tissues (tumor) of MRI brain images with tumor

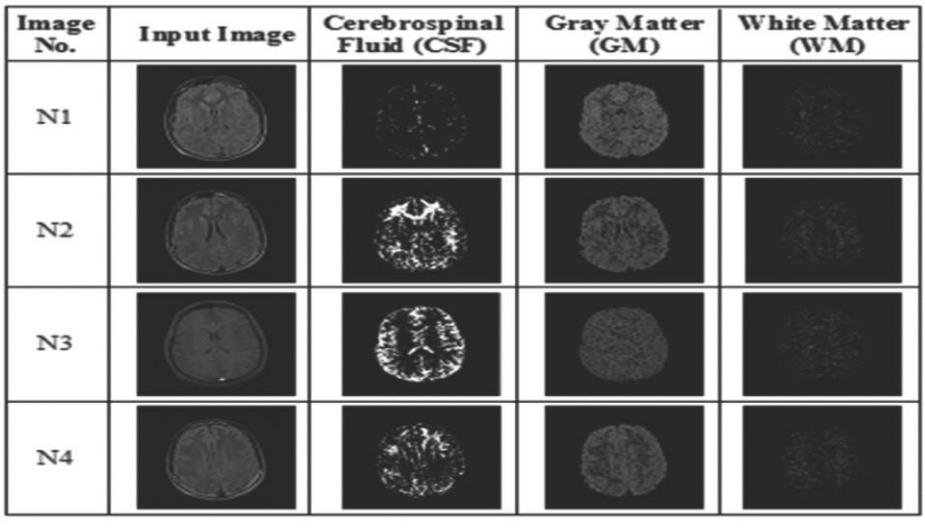

Fig. 5: Segmented normal tissues (CSF, GM, WM) and pathological tissues (tumor) of mri brain images without tumor

The segmentation result is evaluated with the help of quality rate given as follows,

$$\text{Quality rate, } q_r = area(A \cap B) / area(A \cup B) \quad (13)$$

The evaluation of brain tumor detection in different images is carried out using the following metrics, (14)

$$\text{Specificity} = TN/(TN+FP) \quad (15)$$

$$\text{Accuracy} = (TN+TP)/(TN+TP+FN+FP) \quad (16)$$

Where, TP stands for True Positive, TN stands for True Negative, FN stands for False Negative and FP stands for False Positive. Table 2 defines the relevant terms of the evaluation metrics like TP, FP, FN, and TN.

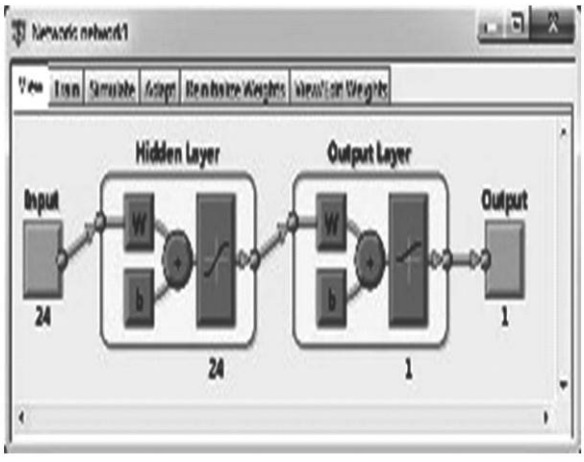

Fig. 6 : Structure of MLRPNN

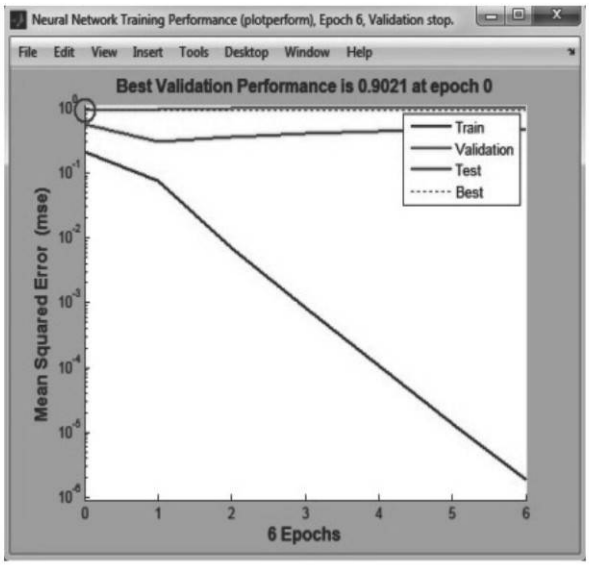

Fig. 7 : Performance validation of MLRPNN

Table 1: Feature values extracted from segmented tissues of MRI brain images

Image No.	Tissue	Feature Values					
		Mean	Var	Ent	Energy		
					Hor	Ver	Diag.
AN1	CS	0.43	0.157	0.7	1.67	1.60	1.32
	GM	68.41	819.2	0.4	12.6	12.1	9.67
	W	33.9	1311.	0.7	15.7	15.2	13.05
	Tu	180.4	1609.	0.3	20.9	12.2	7.2
AN2	CS	0.46	0.14	0.6	1.63	1.60	1.34
	GM	66.87	946.9	0.4	13.3	12.4	10.2
	W	37.13	1369.	0.7	15.9	15.0	13.01
	Tu	181.48	935.0	0.1	12.6	11.7	7.80
AN3	CS	0.51	0.14	0.6	1.58	1.53	1.14
	GM	69.40	861.8	0.4	12.9	11.9	9.62
	W	35.48	1315.	0.7	16.0	15.0	13.01
	Tu	151.10	829.2	0.2	12.2	11.7	7.22
AN4	CS	0.49	0.14	0.67	1.54	1.53	1.21
	GM	65.82	895.1	0.47	13.1	12.3	10.03
	W	37.26	1340.	0.72	15.8	14.9	12.96
	Tu	151.1	829.2	0.22	12.2	11.7	7.22
AN5	CS	0.45	0.15	0.68	1.66	1.48	1.18
	GM	67.55	938.7	0.47	13.2	12.3	10.03
	W	36.24	1355.	0.72	15.9	15.1	12.96
	Tu	180.5	925.2	0.17	12.4	11.4	7.51
AN6	CS	0.46	0.15	0.71	1.51	1.55	1.34
	GM	66.23	899.1	0.47	13.0	12.5	9.99
	W	36.67	1348.	0.73	15.6	15.2	12.91
	Tu	151.0	906.3	0.24	11.9	12.1	8.06
N1	CS	0.53	0.14	0.67	1.52	1.5	1.19
	GM	54.40	430.7	0.4	10.7	10.4	8.18
	W	24.21	825.4	0.74	14.3	13.8	11.84
	Tu	41.38	4272.	0.67	23.3	11.7	8.11
N2	CS	0.22	0.13	0.62	1.5	1.52	1.43
	GM	75.30	397.4	0.26	10.2	10.7	7.56
	W	28.22	1077.	0.73	15.2	15.2	12.83
	Tu	91.16	2965.	0.65	18.3	21.5	18.55
N3	CS	0.28	0.14	0.73	1.53	1.52	1.37
	G	86.64	1044.	0.37	12.5	13.0	9.84
	W	52.44	2138.	0.71	17.6	18.0	14.80
	Tu	82.07	2187.	0.60	16.6	16.3	13.67
N4	CS	0.53	0.12	0.62	1.37	1.43	1.17
	G	59.09	380.3	0.36	10.4	11.2	8.00
	W	26.17	750.2	0.73	13.5	13.9	11.57
	Tu	71.41	3648.	0.73	20.5	17.9	19.37

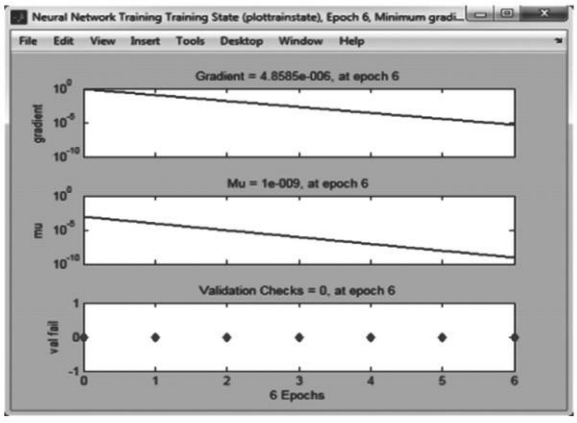

Fig. 8: MLRPNN Training State

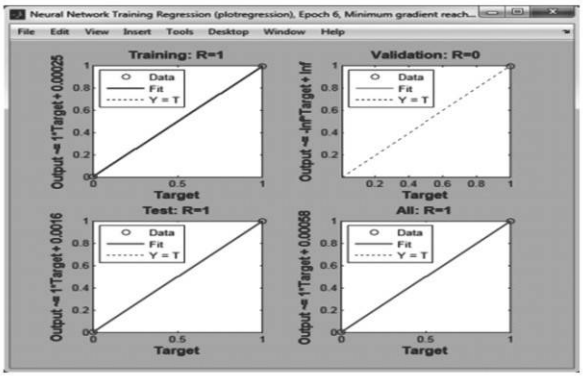

Fig. 9: LRPNN Training Regression Plot

With the aid of the input MRI image training and testing dataset, the values of TP, FP, FN, TN, Sensitivity, specificity and accuracy are given in table III & IV. The results show that the accuracy is 83.33%. The evaluation metrics are also compared with the standard methods like KNN and neural network combined with FCM. The evaluation metrics table shows that our proposed method is more accurate than other two methods.

Table 2: Table defining the terms TP, FP, FN, TN

Experimental Outcome	Condition		Row Total
	Positive	***Negative***	
Positive	TP	FP	TP+FP
Negative	FN	TN	FN + TN
Column total	TP+FN	FP+TN	N=TP+TN+FP+FN

Table 3: Detection accuracy of the proposed method in training dataset

Evaluation Metrics	**Proposed Method (MLRPNN)**	**MLBPNN**	**KNN**	**FCM + NN**
True Negative	50	50	46	46
False Positive	10	10	13	15
True Positive	25	25	22	25
False Negative	5	5	9	4
Specificity	83.33%	83.33%	77.97%	75.41%
Sensitivity	83.33%	83.33%	70.97%	86.21%
Accuracy	**83.33%**	**83.33%**	**75.56%**	**78.89%**
Execution Time (Sec)	**44**	**93**	**88**	**170**

Table 4: Detection accuracy of the proposed method in testing dataset

Evaluation	**Proposed Meth**	**Previous Propo**	**KNN**	**FCM + NN**
	43	43	41	42
	16	16	15	12
False Negat	1	1	2	4
Specificity	100.00%	100.00%	95.35%	95.45%
Sensitivity	94.12%	94.12%	88.24%	75.00%
Accuracy	**98.33%**	**98.33%**	**93.33%**	**90.00%**

The experimental results for normal and abnormal classification are listed in table III and IV. Table IV table shows that our proposed method is more accurate when compared to the other standard

methods. The result showed that MLBPNN and MLRPNN produce the same accuracy. But the execution time of MLRPNN is less when compared to MLBPNN. Once again, MLRPNN was used to classify the abnormal image as benign or malignant. The results for benign or malignant are tabulated in table VI. For our neural network 24-24-10-1, the average execution time is tabulated in table V showing the difference in execution time between MLBPNN and MLRPNN.

Table 5: Average Execution time for 24-24-10-1 NN

Method	Epochs	SD	Execution Time
MLBPNN	114	28	93 sec
MLRPNN	23	3	44 sec

Table 6: Tumour Classification

Type	Benign	Malignant
Benign	39	2
Malignant	1	29

6. Conclusion

In this paper, an effective neural network classifier to identify normal and abnormal (Benign or Malignant) brain images are presented. 150 images (40 normal, 60 malignant and 50 Benign) images are taken. The performance of the proposed technique is evaluated by means of the evaluation metrics namely, Sensitivity, Specificity and Accuracy. The comparative analysis is also carried out with standard methods like KNN, FCM+NN and with our previously proposed method. Current proposed method (MLRPNN) produced the same accuracy as previously proposed method (MLBPNN) but the execution time is twofold reduced. The obtained result shows that the proposed method produces better results than the other classifiers in terms of accuracy as well as in terms of execution time.

References

[1] Selvaraj.,D., Dhanasekaran,R., " Novel approach for segmentation of brain magnetic resonance imaging using intensity based thresholding", 2010 IEEE international conference on communication control and computing technologies, pp 502-507, 7-9 October [2010].

[2] Selvaraj.,D., Dhanasekaran,R., " Segmenting internal brain nuclei in MRI brain image using morphological operators", 2010 International conference on computational intelligence and software engineering, pp 1-4, 10-12 December [2010].

[3] C. A. Parra, K. Iftekharuddin and R. Kozma, "Automated brain data segmentation and pattern recognition using ANN," in the Proceedings of the Computational Intelligence, Robotics and Autonomous Systems (CIRAS 03), December, [2003].

[4] I. Middleton and R. Damper, "Segmentation of Magnetic Resonance Images using a combination of Neural Networks and Active Contour Models," in Medical Engineering & Physics, No. 26, pp. 71-86, [2004].

[5] Zavaljevski, A. Dhawan, A.P. Gaskil, M. Ball, W. and Johnson, J.D., "Multi-level adaptive segmentation of multiparameter MR brain images", Comput Med Imag Graphics, vol. 24, pp. 87–98, [2000].

[6] Suckling, J. Sdsson, T. Greenwood, K. and Bullmore, E.T., "A modified fuzzy clustering: algorithm for operator independent brain tissue classification of dual echo MR images", Magn. Reson. Imag., vol. 17, pp. 1065–1076. [1999].

[7] Alirezaire, J. Jernigan, M.E. and Nahmias, C., "Automatic segmentation of cerebral MR images using artificial neural networks", IEEE Trans Nucl Sci, vol. 45, pp. 2174–2182, [1998].

[8] Nakazawa, Y. and Saito, T. Region extraction with standard brain atlas for analysis of MRI brain images", Proceedings of the IEEE International Conference on Image Process, vol.1, pp. 387–91, [1994].

[9] Clark, M.C. Hall, L.C. Goldgof, D.B. Velthuizen, R. Murtagh, F.R. and Silbiger, S.,"Automatic tumor segmentation using knowledge-based techniques", IEEE Trans. Med. Imag., vol. 17, pp. 187–201. [1998].

[10] Duta, N. and Sonka, M., "Segmentation and interpretation of MR brain images: an improved active shape model", IEEE Trans. Med. Imag., Vol. 16, pp. 1049–1062, [1998].

[11] Suri, J., "Two-dimensional fast Magnetic Resonance brain segmentation", IEEE Eng Med Biol, pp. 84–95, [2001].

[12] Chen, Y. Dougherty, E.R. Totterman, S.M. and Hornak, J.P., "Classification of trabecular structure in magnetic resonance images based on morphological nulometries", Magn. Reson. Med, vol. 29, pp. 358–370, [1993].

[13] Antalek, B. Hornak, J.P. and Windig, W., "Multivariate image analysis of magnetic resonance images with the direct exponential curve resolution algorithm (DECRA). Part 2. Application to human brain images", J. Magn. Reson., vol. 132, pp. 307–315. [1998].

[14] Andersen, A.H. Zhang, Z. Avison, M.J. and Gash, D.M., "Automated segmentation of multispectral brain MR images", J. Neurosci Methods, vol. 122, pp. 13–23. [2002].

[15] T.K. Moon, "The Expectation Maximization Algorithm", IEEE Signal processing magazine, [1996].

[16] T. Logeswari and M. Karnan, "An improved implementation of brain tumor detection using segmentation based on soft computing", Journal of Cancer Research and Experimental Oncology Vol. 2, No: 1, pp. 006-014, March, [2010].

[17] A.W. Toga, P. M. Thompson, M. S. Mega, K. L. Narr, R. E. Blanton, "Probabilistic approaches for atlasing normal and disease-specific brain variability, Anatomy and Embryology", Vol: 204, No: 4, pp: 267–282, [2001]

[18] "Regionprops Algorithm" from http://www.mathworks.in/help/toolbox/images/ref/regionprops.html

[19] Carlos A. Parra, Khan Iftekharuddin and Robert Kozma, "Automated Brain Data Segmentation and Pattern Recognition Using ANN", Computational Intelligence, Robotics and Autonomous Systems (CIRAS 03), December [2003].

[20] D. Selvaraj, R. Dhanasekaran, "Segmentation of cerebrospinal fluid and internal brain nuclei in brain magnetic resonance images," IRECOS, Vol.8, issue 5, pp.1063-1071. [2013]

[21] M.Riedmiller and H.Braun. "A direct adaptative method for faster back propagation learning: the rprop algorithm.", IEEE international conference on Neural Networks, pp. 586-591. [1993].

Fabrication of Hydrogen Peroxide Biosensor based on Thionine Blue and Carbon Nano Tube Modified Glassy Carbon Electrode

A.K. Upadhyay*, Vishakha* and Fathilah Binti Ali**

A highly sensitive and selective multiwalled carbon nanotube based hydrogen peroxide biosensor has been fabricated. The classical redox dye Thionine blue (TB) as mediator and horseradish peroxidase as a base enzyme were coimmobilized into the multi walled carbon nanotubes (MWCNTs) modified ormosil matrix. Nafion was inserted into the ormosil matrix to enhance the rate of the electron transfer and prevent the cracking of modified electrode. Cyclic voltammetry and amperometry measurements were used to study and optimize the performance of the resulting peroxide biosensor. The fabricated biosensor demonstrated significant electrocatalytic activity for the reduction of hydrogen peroxide with wide linear range from 1x10-6 to 3.8x10-4, and low detection limit 1x10-6 M (S/N=3) with fast response time <5 sec.

Keywords: Thionie blue, HRP, Ormosil, Nafion, MWCNTs.

1. Introduction

Carbon nanotubes have emerged as promising nanomaterials for the fabrication of electronic devices and sensor due to their extraordinary physical and electrical properties such as high tensile strength, high elastic modules, high thermal conductivity and electrical conductivity [1, 2]. Unique electrical properties together with high surface area ($300m^2/g$) make them an important component in sensing applications. MWCNTs have been extensively used in the fabrication of electrochemical biosensors due to their excellent electrocatalytic activity and antifouling properties [3-6]. The determination of hydrogen peroxide (H_2O_2) is extensively studied in clinical diagnostics, chemical and pharmaceutical industry and environmental control. Several numbers of MWCNTs modified amperometric peroxide biosensors have been fabricated based on MWCNT/TH/Nf modified PIGE [7], CNT/CHIT/HRP/SG modified GCE [8], MWCNT/HRP/Au modified electrode [9], poly(TB)/HRP/MWCNT/CHIT modified electrode [4]. A series of water soluble Organic dyes such as brilliant cresyl blue [10], methylene green [11], meldola blue [12], Prussian blue [13] and Celestine Blue [14] have been used for the modification of electrode surface and they exhibit excellent mediating ability for the electrocatalytic reduction of H_2O_2. We used Thionine blue (TB) a phenoxazine dye in our investigation due to its higher sensitivity and mediating ability toward H_2O_2 determination. In present work, for the first time we coimmobilized a phenoxazine dye Thionine blue with HRP into the multiwalled carbon nanotubes modified nanoporous ormosil matrix (3-Aminopropyltrimethoxysilane and 2-(3,4-epoxycyclohexyl)ethyltrimethoxysilane) for the development of an amperometric hydrogen peroxide biosensor. Ormosils are used as matrix to encapsulate the enzyme due to its inertness and excellent optical properties. Because of the unique ion exchange, discriminative and biocompatible properties, nafion was dispersed into the matrix to prevent the cracking and brittleness of the modified film [15].The experimental results showed that the MWCNT/TB/NAF/HRP modified GCE exhibited excellent electrocatalytic activity towards the reduction of H_2O_2. The proposed hydrogen peroxide biosensor exhibited better wide linear range and low detection limit toward to H_2O_2.

*Department of Chemistry, College of Engineering, Teerthanker Mahaveer University, Moradabad, India-244001

**Department of Biotech Engineering, International Islamic University Malaysia, Jalan Gombak, Kuala Lumpur, Malaysia-53100

Email: up.arun@gmail.com